cannula, connected to a three-way stopcock via a 20-cm length of PE-50 tubing filled with 0.9% saline. The injections were made slowly (10-15 s), and the injection apparatus was subsequently flushed with 0.4 mL of 0.9% saline. The above measurements were made continuously except for monitoring the isoflurane concentration via the anesthetic agent monitor (Puritan-Bennett).

Acknowledgment. We thank Aaron Carter and Greg Haynes (mouse hot plate) of the University of Maryland and Sarah Harris and Elina Messineo (rat hot plate and tail flick) of Anaquest. We are also thankful for the valuable discussions during manuscript preparation and for the chemical intermediates provided by Dr. Jerome R. Bagley.

Registry No. **5a**, 1155-57-3; **5b**, 120656-71-5; **5c**, 122822-94-0; **6a**, 968-86-5; **6b**, 120070-56-6; **7a**, 122822-95-1; **7b**, 120656-72-6; **7c**, 122822-96-2; **7d**, 120517-22-8; **7e**, 120517-23-9; **7f**, 120115-93-7; **7g**, 120517-24-0; **7h**, 120517-25-1; **7i**, 120517-26-2; **7j**, 120517-29-5; **7k**, 120517-30-8; **7l**, 122823-29-4; **7m**, 122823-30-7; **8a**, 122822-97-3; **8b**, 120656-73-7; **8c**, 122823-20-5; **8c**, 122823-25-0; **8e**, 122823-26-1; **8f**, 120070-49-7; **8f** oxalate, 122823-27-2; **8g**, 122823-28-3; **8h**, 122823-31-8; **8i**, 122823-32-9; **8j**, 121879-86-5; **8k**, 122823-33-0; **9a**, 122823-21-6; **9b**, 122823-22-7; **9c**, 122823-23-8; **9d**, 122823-34-1; **9e**, 122823-35-2; **9f**, 120115-94-8; **9g**, 122823-36-3; **9h**, 122823-37-4; **9i**, 122823-38-5; **9j**, 121879-87-6; **9k**, 122823-39-6; **13**, 120448-97-7; **13** oxalate, 122822-98-4; **14**, 120656-89-5; **14** oxalate, 122822-99-5; **15**, 120657-01-4; **15** oxalate, 122823-00-1; **16**, 120656-91-9; **16** oxalate, 122823-01-2; **17**, 120657-03-6; **17** oxalate, 122823-02-3; **18**, 122823-03-4; **18** oxalate, 122823-04-5; **19**, 120657-07-0; **19** oxalate, 122823-05-6; **20**, 120656-74-8; **20** oxalate, 122823-06-7; **21**, 120656-81-7; **21** oxalate, 122823-07-8; **22**, 122823-08-9; **22** oxalate, 122823-09-0; **23**, 122823-10-3; **23** oxalate, 122823-11-4; **24**, 120657-09-2; **24** oxalate, 122823-12-5; **25**, 120656-96-4; **25** oxalate, 122823-13-6; **26**, 120656-98-6; **26** oxalate, 122823-14-7; **27**, 120657-11-6; **27** oxalate, 122823-15-8; **28**, 122823-18-1; **28** oxalate, 122844-67-1; **29**, 122823-19-2; **29** oxalate, 122844-68-2; **30**, 121879-88-7; **30** oxalate, 121879-89-8; **31**, 121879-90-1; **31** oxalate, 121879-91-2; **32**, 121879-92-3; **32** oxalate, 121879-93-4; **33**, 121879-94-5; **33** oxalate, 121879-95-6; **34**, 121879-98-9; **34** oxalate, 121879-99-0; **35**, 121879-96-7; **35** oxide, 121879-97-8; **36**, 120072-10-8; **36** oxalate, 120072-11-9; **37**, 120072-12-0; **37** oxalate, 120072-13-1; **38**, 120072-14-2; **38** oxalate, 120072-15-3; **39**, 120072-16-4; **39** oxalate, 120072-17-5; **40**, 120070-50-0; **40** oxalate, 120152-15-0; **41**, 122823-16-9; **41** oxalate, 122823-17-0; **42**, 120072-24-4; **42** oxalate, 120072-25-5; **43**, 120072-06-2; **43** oxalate, 120072-07-3; **44**, 120072-26-6; **44** oxalate, 120072-27-7; **45**, 120072-08-4; **45** oxalate, 120072-09-5; **46**, 120071-99-0; **46** oxalate, 120072-00-6; **47**, 120072-01-7; **47** oxalate, 120072-02-8; **48**, 120070-51-1; **48** oxalate, 120072-03-9; **49**, 120072-04-0; **49** oxalate, 120072-05-1; **50**, 120072-28-8; **50** oxalate, 120072-29-9; **51**, 120072-18-6; **51** oxalate, 120072-19-7; **52**, 120072-20-0; **52** oxalate, 120072-21-1; **53**, 120072-22-2; **53** oxalate, 120072-23-3; *o*-$FC_6H_4NH_2$, 348-54-9; $PhNH_2$, 62-53-3; *o*-$ClC_6H_4NH_2$, 95-51-2; $PhCH_2CH_2Br$, 103-63-9; 1-(2-bromoethyl)-4-ethyltetrazol-5-one, 84501-67-7; 2-thiazolyllithium, 40610-14-8; 2-lithio-4-methylthiazole, 89602-38-0; 2-lithio-4,5-dimethylthiazole, 122823-24-9; 2-pyridinyllithium, 17624-36-1; 2-furanyllithium, 2786-02-9; 2-thienyllithium, 2786-07-4; 2-(2-bromoethyl)thiophene, 26478-16-0; 3-(2-bromoethyl)thiophene, 57070-76-5; 1-(2-bromoethyl)pyrazole, 119291-22-4; 2-(2-bromoethyl)pyridine, 39232-04-7; 3-(2-bromoethyl)-2,3-dihydrobenzoxal-2-one, 27170-93-0; 2-(2-bromoethyl)-3-methylthiazole, 671-24-9; 1-(2-bromoethyl)-2-methyl-5-nitro-1*H*-imidazole, 6058-57-7; 1-(2-bromoethyl)-4-iodopyrazole, 122823-40-9; 1-(2-bromoethyl)-3,5-dimethylpyrazole, 67000-35-5; 1-[2-(tosyloxy)ethyl]pyrazole, 80200-20-0; 1-benzyl-4-piperidone.

Supplementary Material Available: Tables listing the final atomic positional parameters, atomic thermal parameters, and bond distances and angles of compound **20**, $C_{25}H_{31}N_6FO_2$ (11 pages). Ordering information is given on any masthead page.

Selective Elimination of Interactions: A Method for Assessing Thermodynamic Contributions to Ligand Binding with Application to Rhinovirus Antivirals

Wan F. Lau and B. Montgomery Pettitt*,†

Department of Chemistry, University of Houston, Houston, Texas 77204-5641. *Received January 5, 1989*

A new method for evaluating the free energy of various physical interactions, such as hydrogen-bond, electrostatic, or van der Waals interactions, is presented. Rather than destroying or creating whole groups, selective (pairwise) interactions are eliminated from the total potential energy and the energy difference with the fully interacting system is evaluated. The exponential ensemble average of such an energy difference is then directly related to the corresponding free energy difference. This procedure is then applied to a rather large protein-ligand system involving the coat proteins of a human rhinovirus and an antiviral ligand. The results seem to indicate that a particular bent hydrogen bond between the ligand and protein system may not be favorable for binding. The method presented gives an estimate of the hydrogen bond free energy contribution with an available trajectory that was previously computed without the expenditure of sizeable computational resources such as recomputing a trajectory. This procedure is effective and efficient for computing the free energy for a given type of physical interaction. It can be used for calculating the binding energy differences for various interactions which can be used to guide the search for isosoluble synthetic targets.

I. Introduction

Many interactions may contribute to the binding of a ligand to a macromolecule. These include electrostatic, van der Waals (dispersion) and, often, hydrogen-bond interactions. Of these various interactions, the requirements for satisfying the potential hydrogen bonds between the protein and its ligand are frequently considered to be among the most important in designing new analogous ligands. If a ligand forms favorable hydrogen bonds with a solvent, and is thereby soluble, it is often reasonable to assume that for a favorable free energy change upon binding there will have to be a compensating number of similar interactions at the binding site. Otherwise, it seems that the equilibrium for binding would be driven in an unfavorable direction. In this work we present a seemingly counterintuitive example where the scenario just mentioned apparently does not hold, when viewed in its simplest form, because the hydrogen bond in question is bent, thereby causing unfavorable interactions with the antecedent atoms involved in the hydrogen bond.

We have earlier attempted to calculate the difference in the free energy of binding between the antiviral WIN52084 and a desmethyl analogue to the coat proteins

† Alfred P. Sloan Fellow 1989-1991.

0022-2623/89/1832-2542$01.50/0

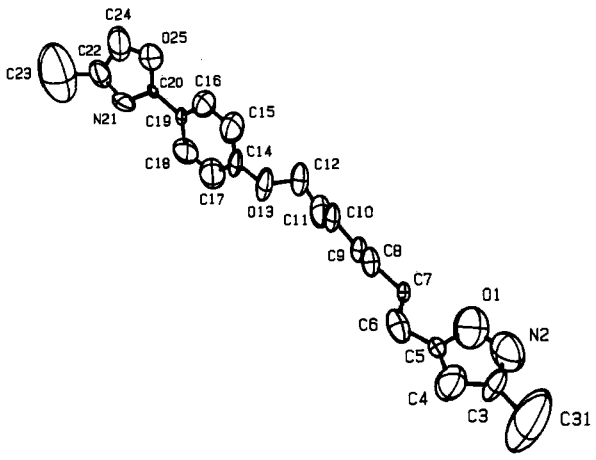

Figure 1. Structure of the antiviral compound 5-[7-[4-(4,5-dihydro-4-methyl-2-oxazolyl)phenoxy]heptyl]-3-methylisoxazole.

of the human rhinovirus-14 (HRV-14).[1] In order to theoretically assess the affinity of a ligand for its protein receptor, it is necessary to accurately calculate the change in free energy on taking the ligand from a solvent to a protein environment. While this remains a difficult theoretical and computational challenge, it is straightforward, though tedious and computationally demanding, to calculate the change in such a free energy difference on making a "small" change in either the ligand or the protein.[2-5,17] Here, we report the use of a new and different technique to estimate the contributions of a single interaction, in this case a hydrogen bond, to the free energy difference of binding and apply the method to an antiviral that binds to the human rhinovirus coat proteins. The structure of the antiviral ligand is shown in Figure 1. The nitrogen on the oxazole end of the ligand is proximal to the hydrogen on the amide group of an Asn residue at the binding site,[6] suggesting the possibility of a hydrogen bond that may function to orient and help bind the oxazole end of the drug.

In the following section, we include a discussion on the estimation of the static binding energy and the approach of selective elimination of electrostatic pair interactions that is developed to estimate the hydrogen-bond contribution to the free energy of binding. This approach will first be tested on a simple model system consisting only of the Asn residue and the hydrogen-bonding fragment of the ligand in order to determine which of the electrostatic pair interactions would best model the hydrogen bond. These interactions are subsequently eliminated in order to mimic the loss of a hydrogen bond. The method is then used on the actual protein–ligand complex. From this "static" estimate of the hydrogen-bond contribution, the approach, in conjunction with well-known formulas from statistical thermodynamics, is finally applied to a dynamic trajectory of the ligand–protein complex in order to determine the free energy contribution of the hydrogen-bond interaction to the binding energy. Such a scheme eliminates the need for computing the isolated solvation contribution to the free energy[17] for the species because the actual solutes are not changing. The overall strategy for a new synthetic target is thus ultimately based on the search for isosoluble compounds which retain or lack certain specific interaction moieties.

In the third section, the results of these studies are presented. We then conclude this paper with a discussion of the results.

II. Methods

The calculations were performed with a modified version of the Charmm program. The dynamic simulation methodology and the general form of the potential functions were as described elsewhere.[7] No explicit hydrogen-bond potential was used; instead, it is assumed to be adequately accounted for by the Coulomb and Lennard–Jones terms. In both the minimizations and dynamics, the nonbonded interactions were calculated with a constant dielectric of 1.0, with a cutoff distance of 8.5 Å. In addition, an interaction switching function with an "on" distance of 7.0 Å and an "off" distance of 8.0 Å was used. Polar hydrogen atoms were explicitly included in the simulations. There were 7639 atoms (or 804 residues) in the apoprotein and 7665 atoms in the holoprotein structures. For the dynamics, the Verlet algorithm was used[15] and shake[16] was applied to the hydrogens. Using a time step of 0.001 ps, the nonbonded list was updated every 10 steps, and coordinates and statistics were collected every 10 steps. The minimized protein structure was heated slowly from 100 to 300 K in 10-deg increments every 200 steps over a period of 4 ps. The protein was then equilibrated at 300 K for 2 ps, with velocity scaling every 200 steps, and then equilibrated without intervention for a further 7 ps. After equilibration, a 10-ps trajectory was collected. The simulation was performed in a microcanonical ensemble (N, V, E) without any velocity scaling. From the trajectory, 1000 coordinate sets at 0.01-ps intervals were collected.

A. Estimation of the Binding Energy. There are several levels of approximation that may be employed in making estimates of the binding energy for a given ligand or moiety within the ligand. Our interest here will be focused, however, on a given interaction, i.e., a hydrogen bond. To estimate the role of a hydrogen bond, as opposed to an atom or group of atoms, requires a different strategy. Recently, the relative free energy of binding was calculated for a pair of phosphonamidate and phosphonate ester inhibitors,[8] complexed with the enzyme thermolysin, by means of a thermodynamic simulation method.[17] The main change was at the site where an oxygen ($q_O = -0.451$) was substituted for the amide group NH ($q_N = -0.705$, $q_H = 0.227$) on the leucine attached to the phosphate while the charge on nearby atoms changed by less than 0.1 e^-. The calculated difference in the free energy of binding was 4.21 ± 0.54 kcal/mol, which compared well with the experimental value of 4.0 kcal/mol.[9] In this procedure, entire atoms were changed, making it conceptually difficult to partition the effects into conventionally physical caricatures of the interactions, such as hydrogen bonds, to give

(1) Lybrand, T. P.; Lau, W. F.; McCammon, J. A.; Pettitt, B. M. Molecular Dynamics Studies of Antiviral Agents: Thermodynamics of Solvation and Binding In *Protein Structure and Design*; UCLA Symposia on Molecular and Cellular Biology, New Series, D. Oxender, Ed., Alan R. Liss: New York, 1987; Vol 69, p 227.
(2) McCammon, J. A.; Tembe, B. L. *Comput. Chem.* **1984**, *8*, 281.
(3) Wong, C. F.; McCammon, J. A. *J. Am. Chem. Soc.* **1986**, *108*, 3830.
(4) Postma, J. P. M.; Berendsen, H. J. C.; Haak, J. R. *Faraday Symp. Chem. Soc.* **1982**, *17*, 55.
(5) Singh, U. C.; Brown, F.; Bash, P. A.; Kollman, P. *J. Am. Chem. Soc.* **1987**, *109*, 1607.
(6) Smith, T. J.; Kremer, M. J.; Luo, M.; Vriend, G.; Arnold, E.; Kamer, G.; Rossmann, M. G.; McKinlay, M. G.; Diana, G. D.; Otto, M. J. *Science* **1986**, *233*, 1286.
(7) Brooks, B. R.; Bruccoleri, R. E.; Olafson, B. D.; States, D. J.; Swaminathan, S.; Karplus, M. *J. Comput. Chem.* **1983**, *4*, 187.
(8) Bash, P. A.; Singh, U. C.; Brown, F. K.; Langridge, R.; Kollman, P. *Science* **1987**, *235*, 574.
(9) Bartlett, P. A.; Marlowe, C. K. *Science* **1987**, *235*, 569.

Table I. Contributions to the Binding Energy

structure	internal energy type	internal energy, kcal/mol
I protein–ligand complex	E_{tot}	−18 201.01
(crystal structure)	E_{enz}	−18 346.74
	E_{lig}	79.99
II protein–ligand complex	E_p^b	−70 676.53
(minimized)	E_l^b	45.26
III protein[a]	E_p^f	−70 745.45
IV ligand[a]	E_l^f	21.46

[a] Minimized structures taken from ref 1.

a precise picture of the cause of this free energy difference.

In this work, we present an alternative method for estimating the hydrogen-bonding energy and free energy. As a reference, however, we shall need an estimate of the binding energy. In a very simple approximate approach, an estimate may be obtained from a series of minimization calculations.[10,17] The interaction energy between protein, p, and ligand, l, E_{pl}, was first calculated from the crystal structure using the formula below:

$$E_{pl} = E_{tot} - (E_{lig} + E_{enz}) \quad (1)$$

where E_{tot}, E_{lig} and E_{enz} are the internal energies of the complex, the ligand, and the protein, respectively.

The estimated binding energy, E_B, may then be calculated from the following equation:[10]

$$E_B = E_{pl} - (E_l^b - E_l^f) - (E_p^b - E_p^f) \quad (2)$$

where E_l^b, E_l^f, E_p^b, and E_p^f are the internal energies of the minimized bound, b, and free, f, ligand and protein, respectively. The calculated binding energy was −27.0 kcal/mol versus vacuum. The energy components of the binding energy analysis are listed in Table I.

B. Estimation of the Hydrogen Bond Stabilization Energy. The calculation of the hydrogen bond stabilization energy is somewhat more complex. The hydrogen bonding aspects of the interaction must be distinguished from other interactions in the system, especially those which are attractive. The force for the majority of H bonds is essentially electrostatic in nature,[11] yet many other forces, such as other dipolar attractions in the system, are also electrostatic. Hydrogen bonds, however, are generally considered to be localized to the vicinity of special moieties. The donor proton in a polar hydrogen bond, $X^{\delta-}\cdots H^{\delta+}$, is attracted to the partially negatively charged polarizable acceptor atom, $X^{\delta-}$. Hence, it might be thought that it is possible to simulate the loss of the H bond by switching off the electrostatic potential terms that contribute to that bond. However, in such a case where hydrogen bonding is modeled by electrostatic interactions, a substantial error in the energy estimate would be incurred by just eliminating the partial charges on either the donor, the acceptor, or both. This is due to the nature of the interactions of those atoms with the surrounding partial charges in the proteins and/or solvent environment. A free energy change of several kilocalories/mole may be found for the destruction of charges or dipoles in such media.[12] Such an effect could overwhelm the single, directional hydrogen-bonding interaction of interest. Therefore, we have chosen to selectively modify the individual pair interactions

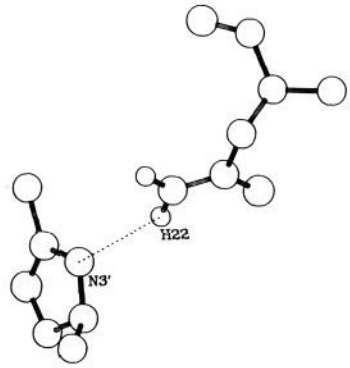

Figure 2. Configuration of the hydrogen bond between an Asn residue and the oxazole fragment of the antiviral ligand. The hydrogen bond is linear and the two residues are nearly coplanar.

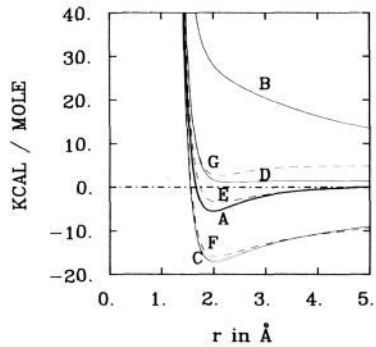

Figure 3. Change in total energy of the hydrogen-bonded Asn and oxazole fragment as a function of the $H^{\delta22}$–N^3 distance. Case A: all electrostatic interactions are included. Cases B–G: selective elimination of electrostatic pairs. Refer to discussion in text.

responsible for the hydrogen bond of interest, leaving the interaction of the donor and acceptor charges, as well as packing effects, with the rest of the system unchanged. Practically in a calculation, as a list of possible interacting pairs is usually kept (and periodically updated), one simply neglects the calculation of the donor–acceptor pairs in the calculation of the electrostatic contribution to the total energy. In order to obtain consistent results, one might postulate that the pairs of interactions to be eliminated should form a nearly neutral set of dipoles to globally balance the coulomb interactions. This arises, in part, because the electrostatic model of a hydrogen bond obtains much of its angular dependence due to repulsions of the primary donor or acceptor atoms with the antecedent atoms on the opposite side. We next demonstrate that several pairs of interactions must be considered an integral part of the hydrogen bonding model interaction.

III. Results

A. Application to a Model System. This simplistic approach was first tested on an elementary system, involving only the Asn residue and the oxazole fragment of the ligand, where the remaining portion of the drug was replaced by a methyl group (Figure 2). The geometry for the test was kept to a linear H bond; i.e., $N^{\delta2}$, $H^{\delta22}$, and N^3 were kept linear. The distance $H^{\delta22}$–N^3 was then changed from 0.5 to 5.0 Å. The change in the total energy of the system as a function of this distance is shown in Figure 3. The plot of curve A shows the resultant potential for the case where all electrostatic interactions were included; curves B–G show the results for the selective elimination of the electrostatic interactions involving the various atoms of the hydrogen bond donor and hydrogen bond acceptor groups. All values are plotted relative to

(10) Pettitt, B. M.; Karplus, M. In *Interaction Energies: Their Role in Drug Design*; Topics in Molecular Pharmacology, Burgen, A. S. V., Roberts, G. C. K., Tute, M. S., Eds.; Elsevier: Amsterdam, 1986; Vol 3.
(11) Pauling, L. In *The Nature of the Chemical Bond*; Cornell University Press: New York, 1960.
(12) Born, M. *Z. Phys.* **1920**, *1*, 45. Kirkwood, J. G. *J. Chem. Phys.* **1934**, *2*, 351.

Table II. Values of the Energies at the Potential Minima and at 5 Å

case[a]	R_{min}[b]	$E_{R_{min}}$	$E_{5.0Å}$
A	1.98	-5.61	0.0
B[c]			13.43
C	2.02	-17.11	-9.04
D	2.28	1.04	1.26
E	2.08	-3.55	-0.18
F	2.10	2.59	4.77
G	2.04	-15.95	-9.42
H	1.84	-50.09	-28.23
I	1.84	-56.27	-33.19

[a] Refer to discussion in the text and to Figure 3. [b] R_{min} is the N–H distance at the minima; $E_{R_{min}}$ and $E_{5.0Å}$ refer to energy at R_{min} and R = 5 Å, respectively. [c] Minimum not observed.

the total energy for case A at 5.0 Å. Quantitative features for the curves are given in Table II. Notice that the total interaction between these molecules (really model fragments) is quite attractive. Thus, the first matter at hand is to identify or characterize the atoms and their associated interactions involved in the hydrogen bond of interest. We proceed by taking the entire set of interactions and then, in stepwise fashion, eliminate those interactions between atoms involved in the hydrogen bonding.

Eliminating only the attractive interactions between the charged atoms $H^{\delta 22}$ and N^3 (curve B) raises the total energy and alters the shape of the curve dramatically with the loss of a minimum at short distance and a large energy at longer distances (see Figure 3 beyond 5 Å). A hydrogen bond is a short-ranged interaction and its contribution should be near zero at larger distances. In addition, the net interaction is too repulsive near the van der Waals contact due to the interactions with the antecedent atoms of the donor and acceptor. Clearly, this restricted set of atoms, the donor–acceptor pair, does not form an acceptable model for the hydrogen bond.

If we consider the three atom set, $N^{\delta 2}$, $H^{\delta 22}$, and N^3 on the oxazole fragment that are involved in the hydrogen bond (curve C), the difference in energy between A and C is +11.5 kcal/mol at the minima. The difference at 5.0 Å of +9.0 kcal/mol indicates that some other attractive interactions should be neglected as well. Curve D is obtained if a second hydrogen, $H^{\delta 21}$, on the Asn is included in the hydrogen-bond set. The difference of -6.6 kcal/mol at the minima is acceptable, but the minima is now at 2.28 Å (compared to 1.98 Å for case A) and the difference at 5.0 Å is -1.3 kcal/mol. However, if the antecedents of N^3 (C^2 and C^4) on the oxazole fragment were also included in the set of eliminated interactions, curve E is obtained, which has a minima at 2.08 Å with a difference of -2.0 kcal/mol at that distance and a difference of only -0.2 kcal/mol at 5.0 Å. This is within the range of a medium strength hydrogen bond.[13] Hence, one has to consider both possible donor hydrogens on the Asn residue and the nitrogen N^3 and its two antecedents in the oxazole ring in order to obtain a reasonable electrostatic representation of the hydrogen bond for this case.

Curve F, which has a minima at 2.1 Å but energy differences of -8.2 and -4.8 kcal/mol compared to those of -2.0 and -0.2 kcal/mol, respectively, for case E, is obtained if only $H^{\delta 22}$ is considered from case D and demonstrates the necessity of including both hydrogens. The antecedent atom C^γ for the Asn residue cannot be included, as shown by case G, where the respective energy differences are now +10.3 and +9.4 kcal/mol due to the fact that the charge

(13) Kaplan, J. G. In *Theory of Molecular Interactions*; Studies in Physical and Theoretical Chemistry, Elsevier: New York, 1986; Vol 42.

Table III. Electrostatic Components of the H bond

	crystal structure		minimized structure	
atom–atom interactions	interaction energy	total	interaction energy	total
1 $N^{\delta 2}$–C^{20}	-46.64	-16.44	-43.30	-21.88
2 $N^{\delta 2}$–N^{21}	46.59		35.56	
3 $N^{\delta 2}$–C^{22}	-16.39		-14.13	
4 $H^{\delta 21}$–C^{20}	24.33	7.70	22.12	10.43
5 $H^{\delta 21}$–N^{21}	-24.81		-18.64	
6 $H^{\delta 21}$–C^{22}	8.18		6.95	
7 $H^{\delta 22}$–C^{20}	27.57	9.95	25.85	13.72
8 $H^{\delta 21}$–N^{21}	-27.19		-20.46	
9 $H^{\delta 22}$–C^{22}	9.57		8.33	
total interaction energy		1.22		2.27

	model system (R = 2 Å)		complex system (R = 2.28 Å)	
atom–atom interactions	interaction energy	total	interaction energy	total
1 $N^{\delta 2}$–C^{20}	-41.11	-12.31	-49.46	-24.58
2 $N^{\delta 2}$–N^{21}	45.04		40.87	
3 $N^{\delta 2}$–C^{22}	-16.24		-15.99	
4 $H^{\delta 21}$–C^{20}	17.39	6.17	25.44	11.49
5 $H^{\delta 21}$–N^{21}	-18.68		-21.78	
6 $H^{\delta 21}$–C^{22}	7.46		7.83	
7 $H^{\delta 22}$–C^{20}	26.90	4.00	29.90	15.93
8 $H^{\delta 21}$–N^{21}	-33.51		-23.56	
9 $H^{\delta 22}$–C^{22}	10.62		9.59	
total interaction energy		-2.14		2.84

on the Asn hydrogen-bond group is no longer neutral. However, the charges of the hydrogen-bond moiety on the oxazole residue is not neutral either, as the charges for the ligand were calculated to maintain molecular neutrality without arbitary segmentation of the charges. The low hydrogen-bond value of -2.0 kcal/mol reflects this charge imbalance as seen from Table III, where the different atom–atom contributions to the hydrogen bond are noted. Table II includes the results for cases H, where the repulsive interactions between the two nitrogens as well as all interactions between $H^{\delta 22}$ and the hydrogen bond dipole interaction with the oxazole are switched off, and I, which includes the interactions in H as well as the corresponding interactions of $H^{\delta 21}$ (see Table III). As seen from the table, these cases, which ignore the repulsions between the hydrogen and the antecedent carbon atoms of N^3, result in differences of +50.1 and +28.2 kcal/mol (for H) and +56.3 and +33.2 kcal/mol (for I) at their respective distances of 1.84 and 5.0 Å. Because of scales used and to avoid overcrowding these curves were not plotted in Figure 3.

The resulting model for the hydrogen bond includes both possible donor hydrogens, which is chemically reasonable as these atoms are both close. The energetic results given above demonstrate that one needs to consider all the interactions involving the dipolar groups and not just the donor hydrogen and the nitrogen acceptor alone nor only those between the donor hydrogen and all of the dipole atoms of the hydrogen-bond acceptor. Hence, case E, where all possible intermolecular electrostatic interactions between the amide nitrogen and hydrogens of Asn and the nitrogen and the following two carbons of the oxazole were selected for elimination, was chosen to represent the loss of the hydrogen bond. This method was then applied to the actual case of the ligand–coat-protein complex.

B. Application on Ligand–Coat-Protein Complex. Table III gives the analysis of the hydrogen-bond energy for the original crystal structure and the minimized complex (100 steps of steepest descent, 100 steps of adopted basis Newton–Raphson to eliminate crystallographic strain

in the structure). The electrostatic interaction energy between the various atoms is listed. It would seem, from the results of Table III, that, if one considers only the interactions involving one hydrogen, $H^{\delta 22}$, which is in a favorable hydrogen-bond position, the resulting stabilization energy is −6.5 kcal/mol for the crystal structure and −9.0 kcal/mol for the minimized structure, which are close to those of the model study for the one hydrogen case (see case F). However, if one were to consider the second hydrogen $H^{\delta 21}$ on the Asn as well, the net interactions of +1.2 and +2.3 kcal/mol for the respective structures indicate an unfavorable contribution from the hydrogen bond involved in the total binding interaction.

Such a result indicates that the net hydrogen-bond interaction with the Asn is unfavorable due to the geometry. Hydrogen bonds are known to have a strong angular dependence as evidenced by both high-level quantum-mechanical calculations as well as classical molecular models derived from both quantum calculations and experimental evidence.[20] The difference found between the complex and the linear model case is thus due to the difference in the orientations of the different residues, as the ligand is apparently unable to assume an optimal position for hydrogen bonding in the binding pocket due to the constraints of its protein environment, as given in the crystallographic data.[6] Hence, we took the actual geometry of the Asn and the ligand from the minimized crystal structure ("complex system") and calculated the changes in the electrostatic, van der Waals, and total energies with respect to changes in the distance between the nitrogen and the hydrogen for this fragment system when all electrostatics are considered, as well as when the hydrogen-bond electrostatic interactions are switched off. This was then compared with a similar analysis for the model (test system) where the hydrogen bond is linear and the two residues are nearly coplanar. The results are given in Figure 4, parts A and B, where the energy changes are plotted for the linear test and the complexed cases, respectively. The values shown for each component were plotted relative to the corresponding values of the fully interacting system (i.e., none of the electrostatics were switched off) for each case.

The linear hydrogen-bond geometry in the test system results in a favorable hydrogen-bond interaction such that the electrostatic component was more negative when all interactions were considered while the geometry implied for the complex system showed the reverse relationship (except at very close distances). Due to its relatively greater electrostatic repulsions, the total energy of the complex system was higher than that for the test system. It is possible that, in this particular example, the protein has tried to minimize its van der Waals repulsive interactions at the cost of increasing electrostatic repulsive interactions for this Asn–ligand pair. The ligand has close van der Waals contact with a large portion of the binding pocket in the X-ray structure, which is also evident in simulation averages.[14] We have not attempted exhaustive quantitative comparisons of the interactions of the ligand with all of the other residues at the binding site to determine how these also might have affected the Asn-ligand interactions.

A comparison of the different interaction energies of the two model systems, linear and complexed geometries, at

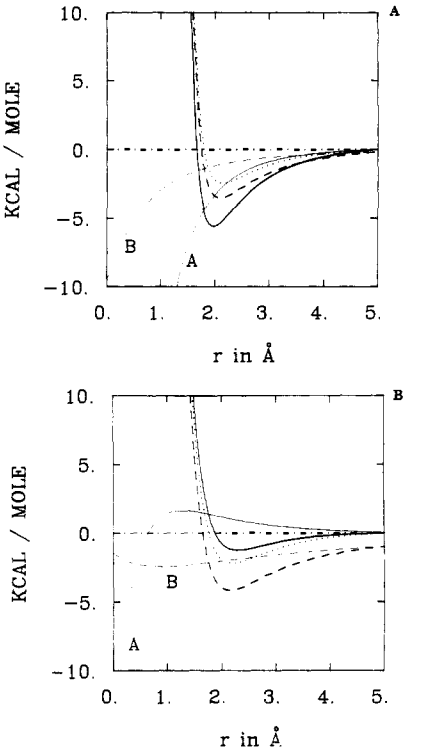

Figure 4. Change in energy components as a function of $H^{\delta 22}$–N^3 distance for test system where hydrogen bond is linear and two residues are nearly coplanar (A) and for the complex system with protein environment orientation (B). Total energy, all interactions included (solid black line); van der Waals energy (dotted line); total electrostatic energy (curve A); and total electrostatic energy minus hydrogen-bond electrostatic interactions (curve B).

their respective energy minima (Table III) indicates that, in the case of the complexed system, the more favorable interactions of $N^{\delta 2}$ of the Asn with the atoms of the oxazole hydrogen bond have been offset by the unfavorable interactions of its hydrogens with the corresponding atoms on the oxazole residue, the major differences being the interactions of the donor hydrogens with C^{20} (especially for $H^{\delta 21}$) and a decreased attractive interaction of $H^{\delta 22}$ with N^{21}. These contributed to a less favorable hydrogen bond type interaction for the complex system. Also, it can be seen from Table III that the interactions with C^{20} dominate over those with C^{22}. This is due to the difference in their charges, with C^{20} being much more positively charged than C^{22} (+0.8319 vs +0.3132).

C. Estimation of the Hydrogen Bond Free Energy Contribution. While interaction energy analyses are traditional in modeling interactions, free energies must be evaluated for chemically relevant and realistic interaction estimates. To test the results of our simple modeling procedure, our method of selective elimination of interactions combined with statistical thermodynamics was applied to a 10-ps dynamics trajectory of the ligand–protein complex to estimate the free energy of stabilization of the hydrogen bond. The trajectory was obtained from an earlier simulation study on the dynamics of the protein–ligand complex.[14] The total energy of the complex with all interactions (E_{tot}) and minus the hydrogen-bond interactions (E_{nHb}) were calculated for 100 sets of coordinates (i.e., at 0.1-ps intervals). With use of the thermodynamic difference formula obtained from the ratio of the two partition functions (sometimes loosely referred to as the perturbation method[17,18]), the estimated free energy

(14) Lau, W. F.; Lybrand, T. P.; Pettitt, B. M. *Mol. Simul.* **1988**, *1*, 385.
(15) Verlet, L. *Phys. Rev.* **1967**, *159*, 98.
(16) van Gunsteren, W. F.; Berendsen, H. J. C. *Mol. Phys.* **1977**, *34*, 1311.
(17) Brooks, C. L.; Karplus, M.; Pettitt, B. M. *Adv. Chem. Phys.* **1988**, *71*, 1.

difference was calculated. The equation used was

$$\Delta G = RT \ln \langle \exp(-(E_{tot} - E_{nHb})/RT) \rangle_{tot}$$

Application of this formula employing our selective deletion of hydrogen bonding pair interaction contributions gave a value of $+1.58 \pm 0.02$ kcal/mol. This indicates that the conclusions obtained from the simplistic modeling study were reasonable and that the entropic contributions in this case are probably minimal. The standard deviation quoted is only a lower bound on the purely statistical errors.

IV. Conclusions

While it is clear that there is a net attraction between the oxazole fragment and the Asn side chain for all geometries explored in this study, we have found that the hydrogen-bonding part of that total interaction is not necessarily favorable. Given our model and its justification, the hydrogen-bonding contribution as calculated by several methods was small in magnitude. We found the hydrogen bond between Asn 219 and the nitrogen on the oxazole portion of the ligand contributes an unfavorable 1.58 kcal/mol (5.9%) to the binding energy. While the magnitude is certainly model dependent, the trends should be transferable. The result from the dynamics trajectory indicates that during the course of a simulation[14] the ligand was unable to reorient itself to optimally hydrogen bond with the Asn residue. The constraints imposed on it by its protein environment had not been changed even after equilibration and a dynamic trajectory. We also found from our earlier dynamical analysis[14] that the ligand serves as a correlation linker between the residues of the binding site. This linker model for the ligand then implies the presence and maintenance of close contacts with the protein surface at the heterocyclic rings and, hence, the prevention of reorientation of the ligand for favorable hydrogen bonding with the Asn residue. The strength of these constraints can be appreciated from the somewhat bowed conformation of the ligand in the protein–ligand complex X-ray structure versus its linear free form.

It should be mentioned that a number of computational and physical approximations were made in these calculations. The effects on the protein of a solvent bath were not included. The results would probably be qualitatively similar since there is almost no solvent exposure of the bound drug. Also, the change in state for the thermodynamic calculations was carried out in one step, although, in principle, a more gradual change would give more accurate results. However, the total change in free energy was only $2RT$ and, hence, the single-step procedure employed was probably adequate.[10,17] It should be mentioned that the present analysis was an attempt to get a rough estimate of the hydrogen-bond free energy with an available trajectory that we had previously computed without the expenditure of further sizeable computational resources. Thirdly, the thermodynamic difference calculated above was not designed to represent a real experimental case; i.e., it's not possible for the atoms involved to selectively ignore only certain electrostatic pair interactions. However, this procedure is effective and efficient for computing the free energy contribution for a given type of interaction. The above calculations demonstrate how one might theoretically analyze interactions that would not be simply attainable experimentally and, hence, give some insight into possible experiments or simulations to perform. The scheme above eliminates the need for computing the solvation free energy for the solute species, given that one is satisfied with a given class of ligand's delivery characteristics and, therefore, solvation properties. Thus, the scheme proposed for searching for new compounds relies on changing the binding site of the equilibrium and not the solvation side.[17]

For example, one could attempt to find a mutant whose Asn residue has been replaced with another isosteric amino acid that would not have the above antecedent electrostatic interactions. One possibility would be a histidine residue. Although His is similar in structure to Asn and is considered a conservative substitution, it might be poorly accommodated, as found, for the His substitution for Thr 157 in phage T4 lysozyme.[19] Clearly, from the perspective of drug design and antiviral therapy, the design of a more susceptible target would not be a very profitable venture. It would be more useful to design another ligand that would bind better, assuming that biological efficacy correlates with binding potency. The above results point toward several possibilities, all aimed at reducing the positive charge on C^{20} and/or increasing the nucleophilicity of the nitrogen on the oxazole ring, while maintaining the ligand's partition coefficient (bulk solubility difference). An interesting experimental test of the insights derived from our procedure could involve the replacement of the oxazole nitrogen with a nonacceptor atom. We are in the process of carrying out some other relevant calculations for such systems, which will be reported in a later paper.

Acknowledgment. We appreciate many conversations with Professors T. Lybrand, J. A. McCammon, and Dr. A. Tresurywalla. We also thank Prof. M. Rossmann and Dr. J. Badger for communicating X-ray coordinates prior to publication. The authors thank the National Institutes of Health, the Robert A. Welch Foundation, and the Sterling Winthrop Research Institute for financial support of this work. The San Diego Supercomputer Center and the NSF, through our departmental VAX/FPS, provided the computational resources for the project.

Registry No. 5-[7-[4-(4,5-Dihydro-4-methyl-2-oxazolyl)-phenoxy]heptyl]-3-methylisoxazole, 120666-36-6.

(18) McCammon, J. A.; Harvey, S. *Dynamics of Proteins and Nucleic Acids*; Cambridge University Press: Cambridge, 1986.

(19) Alber, T.; Dao-pin, S.; Wilson, S.; Wozniak, J. A.; Cook, S. P.; Matthews, B. W. *Nature* **1987**, *330*, 41.

(20) Jorgensen, W. L.; Chandresekhar, J.; Madura, J. D.; Impey, R. W.; Klein, M. *J. Chem. Phys.* **1983**, *79*, 926. Reiher, W. Ph.D. Thesis, Harvard University, 1985.